Volume 1 | Number 1 | Jan 2013 | Pages 1–100

Analytical Methods

www.rsc.org/methods

ROYAL SOCIETY OF CHEMISTRY

ROYAL SOCIETY OF CHEMISTRY

www.rsc.org/methods

Selected ion flow tube mass spectrometry analyses of laser decomposition products of a range of explosives and ballistic propellants

Svatopluk Civiš[1*], Martin Civiš[1], Kristýna Sovová[1], Kseniya Dryahina[1], Jiří Kubišta,

Petr Skřehot,[2] Patrik Španěl[1] and Martin Kyncl[3]

[1]*J. Heyrovský Institute of Physical Chemistry, Czech Academy of Sciences, Dolejškova 3,*

182 23 Prague 8, Czech Republic

[2] *Safety and Health Expert Institute, Ostrovského 253, 150 00 Prague 5, Czech Republic*

[3] *Explosia a.s., Semtín 107, 530 50 Pardubice, Czech Republic*

Abstract

The rationale of this study was to quantitatively characterise differences and similarities in the gaseous and volatile components of the decomposition products of 38 types of commercially produced explosives and propellants. A combination of laser-induced breakdown (LIB) and selected ion flow tube mass spectrometry (SIFT-MS) methods was used. The surface of the bulk samples was irradiated by a sequence of 10 laser pulses, 150 mJ each, in an argon atmosphere to simulate the explosion or combustion on a microscopic laboratory scale. The gas from the reaction zone was analysed in real time by SIFT-MS. The concentrations of the decomposition products (NH_3, HCN, HCHO, NO, NO_2, HONO, HNO_3, C_2H_5OH, CH_3CN, DMNB, C_2H_6CO, C_2H_2 and nitroglycerine) were determined and statistically processed using multivariate principal component analysis (PCA). The results revealed that there are similarities in the quantitative compositions of the decomposition products for similar explosives and similar propellants. PCA visualisation highlights that characteristic combinations of compounds correspond to the decomposition of nitrocellulose and nitrocellulose-based propellants (including trade mark Lovex), and different combinations correspond to various plastic explosives (trade mark Semtex). The conclusion of this work is that the present methodology can be used for safe and non-destructive studies of characteristic explosion products without the need for the initiation of hazardous quantities of explosives in the form of test charges.

Keywords: Laser-induced Breakdown, Selected Ion Flow Tube Mass Spectrometry, Explosives, PCA,

_____

*Corresponding author, e-mail: Civiš@jh-inst.cas.cz,

Phone: +420-286 591 766

1 Introduction

An understanding of the complex processes involved in the explosive decomposition of energetic material is essential for the development of reliable models for the performance, stability and hazard analysis of explosives. Identification of the decomposition products is of prime importance in identifying toxic, hazardous and environmentally polluting species. The characterization of the decomposition mechanism of energetic materials leads to an increased understanding of the relationship between structure, sensitivity and performance.

Energetic and explosive materials are pure substances or mixtures that chemically react to large amounts of rapidly liberated heat and gas. Today, approximately 150 different formulas are used for the military, commercial, and illicit production of explosives.[1, 2] Energetic materials and explosives may be inorganic or organic in nature and can be divided into two broad categories (low-energy explosives and high-energy explosives) based on how readily a reaction is initiated and its intensity.

Many explosives consist of a fuel component (usually a hydrocarbon) and an oxidizer (typically an oxide of nitrogen), which may be contained within the same molecule. To be of broad utility, a sensing technique needs to have the capability to rapidly detect and identify the wide variety of different constituents that are present in energetic materials and explosives.

One of the most pressing needs for the military is the stand-off detection of explosives. As a result of the drastically reduced sensitivity at increasing distances and the generation of potentially harmful ionization radiation, neither x-ray imaging [3] nor neutron activation [4] is practical at stand-off distances [5]. Although terahertz imaging is a promising technique that employs non-ionizing radiation [6], the absorption of water vapour and other species from the atmosphere could potentially limit its application in stand-off detection [7]. Most trace explosive detection techniques, such as ion mobility spectrometry and gas chromatography [8], rely on vapour detection. Unfortunately, at room temperature, the vapour pressures of many common explosives are extremely small (ppbv or less), and attempts to conceal the explosives by sealing them in packaging materials can decrease the vapour concentrations by as many as three orders of magnitude [9] [7]. Optical techniques such as cavity ring-down spectroscopy (CRDS) [10], Raman spectroscopy [11], photoacoustic spectroscopy [12, 13], and photo fragmentation [14] followed by resonance-enhanced multiphoton ionization (PF-REMPI) or laser-induced fluorescence (PF-LIF) have been applied to trace explosive detection [9]. Of these techniques, only Raman spectroscopy [15] has been demonstrated on solid

explosives at stand-off distances (10 to 50 m), although long integration times (i.e., multiple laser shots) are required to improve the signal-to-noise ratio [16, 17].

An alternative optical technique for the detection of explosives is laser-induced breakdown spectroscopy (LIBS). [18] The ability of LIBS to provide a remote, rapid multi-element micro-analysis of bulk samples (solid, liquid, gas and aerosol) in the parts-per-million range with little or no sample preparation has been widely demonstrated and is the greatest advantage of LIBS compared with other analytical approaches. LIBS holds particular promise for the detection and identification of explosives because of its intrinsic capability for minimally destructive, *in situ*, real-time detection and analysis of chemical species. More recently, the capability of LIBS to identify compounds has been realised with the advent of high-resolution broadband spectrometers. In our previous papers[19, 20], LIBS was used to analyse atomic fragments, short-lived radicals and excited molecules in the visible spectral range. The success of LIBS for identifying organic compounds, based on atomic or molecular emission intensity, led to the investigation of the characteristics of LIBS spectra of explosive (carbon, hydrogen, oxygen, and nitrogen are found in most military explosives) compounds.

A promising method for the analysis of the stable decomposition products of energetic materials is a combination of the laser-induced breakdown (LIB) [21] technique with the selected ion flow tube mass spectrometry (SIFT-MS) technique. The combination of these techniques has been recently presented in our two papers, which present the results of experiments with hexogen, octogen, pentrite, trinitrotoluene[20] and FOX-7 (1,1-diamino-2,2-dinitroethylene)[19] and study the decomposition mechanism of these high-energy materials. The value of such a combination is based on the fact that the macroscopic explosion of large charges is overcome due to the use of LIB (ArF excimer laser (193 nm, 20 ns, and 150 mJ) to initiate the chemistry mimicking that of explosions in microgram amounts. The stable gaseous products resulting directly from the laser initiation are continuously sampled and quantified using SIFT-MS. Selected ion flow tube mass spectrometry (SIFT-MS) [22, 23] linked with LIB has thus been established as a technique to characterise the composition of the volatile products of explosions in small-scale laboratory experiments, without the need to initiate the explosions of test charges weighing several grams or more. In the present study, this combination of LIB and SIFT-MS [19, 20] was used to study the volatile products of the decomposition of microgram amounts of several commercial explosives and propellants, some used as pure compounds and some present in the form of mixtures of energetic materials with additives as listed below.

3

1.1.   Explosives and propellants included in this study

The materials used in this study are representative samples of the Explosia a.s. production, covering a range of diverse chemical compositions and containing pure explosives that were previously studied. The following list defines the abbreviations or trade names of explosives and propellants included in the present study, using the chemical names of the compounds together with their CAS numbers, when available.

Explosives

Azole-based materials

> **ATZ** (5-aminotetrazole-hydrate), $CH_3N_5 \cdot H_2O$ [15454-54-3]
>
> **NTO** (3-nitro-1,2,4-triazole-5-one), $C_2N_4O_3$ [24807-55-4]
>
> **GZT** (Guanidium azotetrazolate), $C_4H_{12}N_{16}$

Guanidine and urea based materials

> **TAGN** (triaminoguanidine nitrate), $CH_9N_7O_3$, [4000-16-2]
>
> **Guanidinium nitrate,** $CH_6N_4O_3$ [506-93-4]
>
> **NQ** (nitroguanidin), $CH_4N_4O_2$ [556-88-7]
>
> **Nitrosourea**, $CH_3N_3O_2$ [684-93-5]
>
> **Urea nitrate,** $CH_5N_3O_4$ [124-47-0]

Cyclic nitroamines

> **HNIW** (2,4,6,8,10,12-hexanitro-2,4,6,8,10,12-hexaazaisowurtzitane) [135285-90-4].

Nitroaromatics

> **Picric acid** (2,4,6-Trinitrophenol) $C_6H_3N_3O_7$ [88-89-1]
>
> **Tetryl** (2,4,6-trinitrophenylmethylnitramine), $C_7H_5N_5O_8$ [479-45-8]

Other nitro compounds

> **TNAZ** (1,3,3-trinitroazetidine) $C_3H_4N_4O_6$ [97645-24-4]
>
> **TEX**   (4,10-dinitro-2,6,8,12-tetraoxa-4,10-diaza-tetracyclo   [5,5,05,9,03,11] dodecane)
>
> **FOX-7** (1,1-diamino-2,2-dinitroethene) $C_2H_4N_4O_4$ [145250-81-3]
>
> **Ammonium nitrate**, NH_4NO_3 [6484-52-2]
>
> **GA** (guanidinium 5-aminotetrazole), $C_2H_8N_8$ [51714-45-5]

Pentaerythritol tetranitrate (PETN) containing mixtures

> **Semtex 10** (PETN, Pentaerithrityl tetranitrate, $C_5H_8N_4O_{12}$ [78-11-5] 85 %, 12,5 % mixture of polybutadien nitrile rubber and dibutyle phthalate 25:75,

4

dibutyl phthalate 1,5 %, DMNB (2,3-dimethyl-2,3-dinitrobutane) $C_6H_{12}N_2O_4$ [3964-18-9] 1%)

Semtex 1A (PETN 83%, 17 % mixture of polybutadiene styrene rubber and mineral oil 30:70, DMNB 0,1 %)

Semtex 1H (PETN 35 %, RDX, 1,3,5-Trinitro-1,3, 5-triazacyclohexane, $C_3H_6N_6O_6$ [121-82-4] 50 %, 15 % mixture of polybutadiene styrene rubber and mineral oil 20:80), DMNB 0,1 %)

Semtex 10SE (PETN 76 %, expanded polystyrene 9%, dibutyl phthalate 10 %, silica 5 %, DMNB 0,1 %)

PETN + wax (PETN 90%, wax 10%).

Industrial explosive for mining

Permonex V19 (ammonium nitrate and Trinitrotoluene (TNT) $C_7H_5N_3O_6$ [118-96-7]).

Propellants

Nitrocellulose

Nitrocellulose A (11.55 % N)

Nitrocellulose B (12.52 % N)

Nitrocellulose C (13,52 % N)

Smokeless propellants

Lovex S011 (nitrocellulose smoke free pistol powder)

Lovex S040 (nitrocellulose smoke free gun powder)

Lovex D073 (nitrocellulose powder, 12 % nitroglycerine)

Lovex SYN (nitrocellulose powder, 50 % nitroglycerine)

Lovex D380 (nitroguanidine powder for guns)

Rocket propellants

A-IX-1 (RDX + wax; artillery ammunition)

TNF (picric acid)

Neva (RDX 75.92 %, triol 24.08 %)

T/H 52/48 (RDX 19.24 %, triol 80.76 %)

3H11M KUB (RDX 79.21 %, triol 20.79 %)

3H12 KUB (RDX 0.08 %, triol 99.92 %)

Volchov 85M (RDX 79.65 %, triol 20.35 %)

> **P73 2520** (nitrocelullose 80 % with 13.1 % of N_2, nitroglycerine 12.5 %, centralit I 4.5 %, akardit II 0.8 %, diphenylamine 0.7 %, sodium sulphate 0.2 %, potassium nitrate 0.5%, graphite 0.4 %).

The names or abbreviations given in bold will be used throughout this article.

2. Experimental section

### 2.1. Sample preparation and experimental protocol

Samples of bulk explosives were prepared in the form of tablets by compressing powders using a tablet press machine to a thickness of 2 mm. The use of tablets of bulk explosives was found to be preferable to the use of thin films on a metallic surface because of the elimination of parasitic metal atom emission and metal particles[20]. An ArF excimer laser (193 nm, 20 ns, and 150 mJ) was used to create pulses of radiation that were focused using a 15 cm quartz lens onto the surface of a rotating target placed in a vacuum chamber filled with Ar at pressure of 1 atm. The stable gas products originating from the plasma generated by ten repeated laser pulses were extracted via a heated calibrated PEEK capillary.

2.2. SIFT-MS

SIFT-MS is a method for the accurate quantification of trace gases using the knowledge of the kinetics of ion-molecule reactions. It is based on chemical ionization using H_3O^+, NO^+ and $O_2^{+\bullet}$ precursor ions that do not react with the major components of air. Absolute quantification in real time is achieved on the basis of first-order kinetics. The absolute concentrations are calculated from the known rate constants, count rates of precursor ions and product ions, the known reaction time and other physical quantities such as the flow rate of the sample, flow rate of helium, flow tube pressure and flow tube temperature. In this study, SIFT-MS was used to quantify stable gaseous products originating from the plasma during an LIB event. A SIFT-MS instrument (*Profile 3* SIFT-MS) manufactured by Instrument Science Limited (Crewe, UK) was used[24, 25]. A sampling PEEK capillary heated to 80 °C connected directly to the SIFT-MS instrument was used to transfer the argon containing the volatile products of decomposition at a regular flow rate of 20 mL/min (see the experimental set-up in Figure 1).

Full scan mass spectra were acquired, whilst the three precursor ions were alternatingly injected into the helium carrier gas in the flow tube where the ion-molecule reactions take place. The range of the mass-to-charge ratio was set to 10-200 m/z, with a total

integration time of 100 s. Concentrations of several compounds (listed in Table 1) were calculated (in parts per billion by volume, ppbv) from the ratios of the count rates of characteristic product ions to the count rates of the precursor ion using a library of kinetic data, as is usual in SIFT-MS analysis [26, 27].
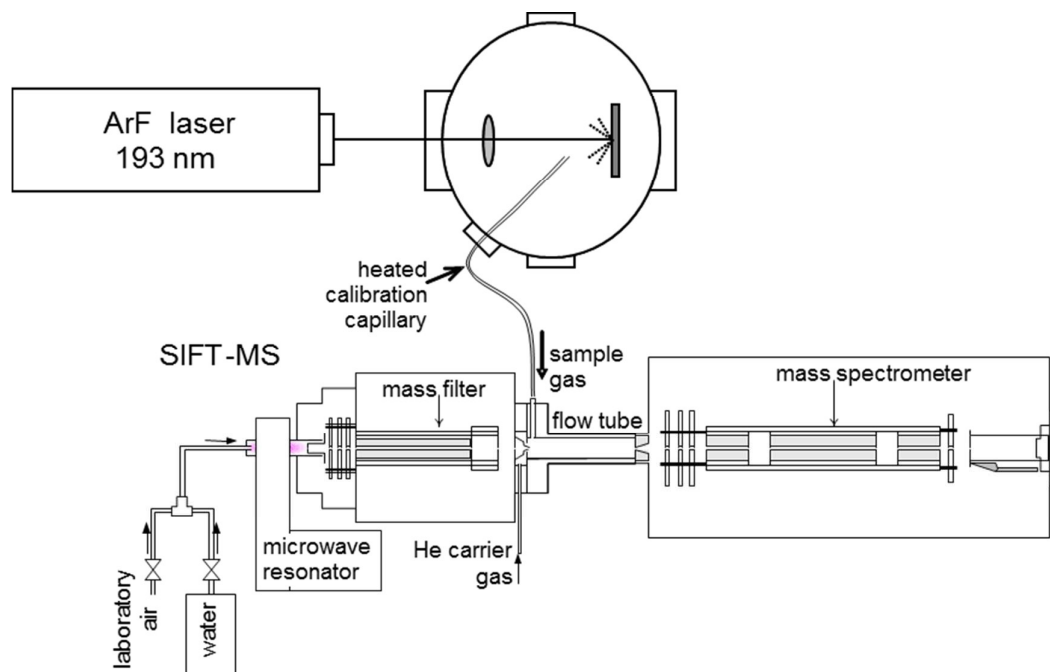
Figure 1 Schematic diagram of the experimental apparatus.

2.3. Statistical analyses

Data on the gas phase concentrations of individual compounds, in ppbv, obtained for all individual explosives and propellants were compiled into a matrix, with rows corresponding to different samples and columns corresponding to individual compounds, and then statistically analysed using the method of principal component analysis, PCA (software Principal component analysis for SIFT-MS 2009 written by Dryahina and Španěl), previously used to analyse data on volatile compounds emitted by bacterial cultures [28].

3. Results and Discussion

3.1 LIB combined with SIFT-MS measurement

The SIFT-MS mass spectra were obtained using the precursor ions H_3O^+ and O_2^+ to ionise gas sampled directly from the reaction zone after the irradiation of the tablet argon atmosphere by the laser pulse. Inspection of these mass spectra revealed the presence of the following stable molecular species: acetone (CH_3COCH_3), acetylene (C_2H_2), acetonitrile (CH_3CN), ammonia (NH_3), dimethyldinitrobutane (DMNB), ethanol (CH_3CH_2OH), formaldehyde (HCHO), hydrogen cyanide (HCN), nitric acid (HNO_3), nitric oxide (NO), nitrous acid (HONO), nitrogen dioxide (NO_2) and nitroglycerine.[29] The mean absolute concentrations of these stable products obtained during the first 10 seconds after the LIB event for the four types of explosives are given in Table 1 in units of parts per billion by volume (ppbv), equivalent to nmol/mol.

1
2
3
4
5
6
7
8
9
10
11
12
13
14
15
16
17
18
19
20
21
22
23
24
25
26
27
28
29
30
31
32
33
34
35
36
37
38
39
40
41
42
43
44
45
46
47
48
49

Table 1 Mean concentrations in parts per billion by volume (ppbv) of the compounds identified by SIFT-MS in the atmosphere inside the experimental chamber during 10 secons following the initiation of the explosive samples using laser pulses.

Sample	Acetone	Acetylene	Acetonitrile	Ammonia	DMNB	Ethanol	Formaldehyde	Hydrogen cyanide	Nitric acid	Nitric oxide	Nitrous acid	Nitrogen dioxide	Nitroglycerine
ATZ	3	9	0	73	0	1142	19	855	28	274	39	307	1
NTO	0	38	1	21	0	375	16	119	24	126	14	75	0
GZT 9	5	8	1	64	0	180	8	800	20	181	4	93	0
TAGN	4	0	0	35	0	462	12	271	12	118	12	88	1
Guanidinium nitrate	3	0	1	21	8	150	39	11	30	553	25	18	2
NQ	27	2	0	73	2	244	65	15	44	559	20	70	4
Nitrosourea	1	0	0	8	0	93	23	6	16	572	8	30	2
Urea nitrate	2	0	0	14	4	140	38	9	33	255	17	30	1
HNIW	12	0	0	42	0	169	19	540	34	1149	16	313	0
Pickric acid	2	0	0	17	3	64	30	8	15	548	6	34	2
Tetryl	6	6	1	29	3	181	38	57	24	907	15	62	3
TNAZ	4	0	0	74	0	284	19	70	9	915	2	118	0
TEX	14	2	0	23	4	101	3	209	12	465	7	43	0
FOX-7	27	3	0	26	7	2110	84	43	32	500	86	151	5
Ammonium nitrate	8	0	1	37	2	113	44	5	14	861	16	59	1
GA	0	0	0	100	0	468	9	484	27	130	11	220	1
Semtex 10	36	0	3	15	72	407	117	116	75	479	29	28	6
Semtex 1A	13	103	3	70	62	302	132	101	62	767	31	87	0
Semtex 1H	22	27	0	30	407	569	140	109	59	996	26	104	5
Semtex 10SE	28	2	3	39	136	165	48	25	35	487	6	60	2
PETN+wax	39	29	3	45	11	256	82	47	27	1009	23	89	1
Permonex V19	5	0	0	19	0	179	4	12	6	112	8	69	0
Nitrocelullose A		0	0	47	3	273	113	32	36	580	50	64	0
Nitrocelullose B	44	2	0	40	2	258	89	15	44	565	85	43	2
Nitrocelullose C	38	6	0	28	5	1069	44	51	29	869	116	62	2

9

|												
Lovex S011	137	0	0	30	6	175	121	3	46	343	19	37	2
Lovex S040	51457	0	0	24	10	302	150	23	52	765	34	146	3
Lovex D073	2746	2	2	25	2	239	65	40	30	636	63	70	3
Lovex SYN	920	0	2	14	5	220	51	0	39	617	47	399	1
Lovex D380	308	0	2	62	14	194	34	78	38	736	27	162	5
A-IX-1	2	21	4	35	5	166	63	301	41	633	23	31	2
TNF	8	0	2	19	4	129	48	54	40	549	19	51	3
Neva	2	5	0	19	6	152	72	115	37	373	30	52	2
T/H 52/48	2	5	4	15	4	153	55	93	36	614	18	49	1
3H11M	5	0	0	21	8	169	46	72	25	873	28	42	0
3H12 KUB	3	12	0	5	4	29	29	92	32	200	4	42	1
Volchov 85M	2	3	0	18	4	131	40	36	20	473	11	7	1
P73 2520	2289	11	1	46	10	779	98	20	36	804	88	85	10

10
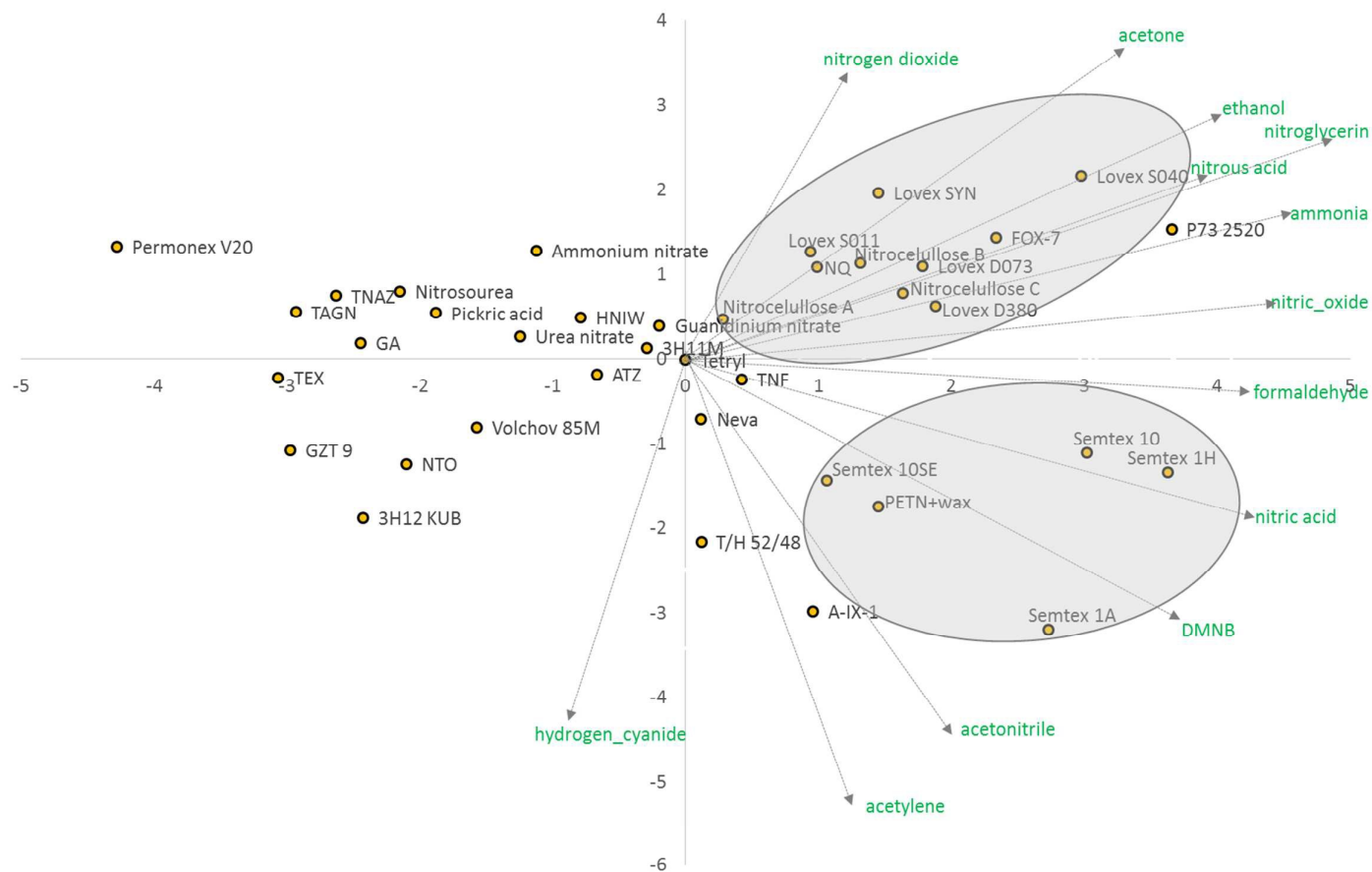
Figure 2 Two dimensional visualisation of the results of the principle component analysis of the concertation data given in Table 1. The arrows illustrate the loadings associated with each of the compounds in relation to the principal components PC1 (x-axis, 26% of the variability) and PC3 (y-axis, 14%). The directions of the arrows correspond to increasing concentrations of the compounds above the mean for all samples. The data points indicate the scores for the individual samples as labelled. The groups of gun propellants and Semtex explosives are indicated by shaded clusters.

MS interpretation and data preparation for PCA statistics

Nine full scan spectra were acquired for each of the 38 explosives using SIFT-MS. The spectral range covered count rates of ions at 190 different m/z values for 3 precursor ions. The obtained spectra were inspected, and 13 volatile compounds were identified as significant components of the volatile decomposition products on the bases of knowledge of the ion chemistry of the 3 precursor ions and experience from previous experiments.

The absolute average concentrations of these compounds were calculated from the ratios of the count rates of the product ions to the count rates of the precursor ions, as described in [26], in a matrix exactly corresponding to Table 1 (38 rows and 13 columns), to be processed by PCA. The results of the PCA analysis of these data were obtained in the form of eigenvectors describing the loadings of individual compound concentrations. The first principal component, PC1, explains 26% of the variability and contains major loadings from all 13 VOCs except hydrogen cyanide. The third principal component, PC3 (14%) has major contributions from hydrogen cyanide, acetonitrile, nitric acid, DMNB and acetylene. The results of the PCA analysis can be used to visualise the variations of the 13 concentrations amongst the samples in a two-dimensional plot, as shown in Figure 2. Note that clear clustering is observed, revealing a distinct group of nitrocellulose-based products (in the direction of NO, NO_2, nitrous acid, nitro glycerine, acetone, and ammonia) and also a group of several types of Semtex (in the direction of DMNB added as a taggant according to the Convention on the Marking of Plastic Explosives (so-called Montreal Protocol) that has been ratified by 152 states).

4. Conclusions

The combined experiments using LIBS and SIFT-MS have allowed for the analyses of the volatile decomposition products of commercial mixtures, and it was demonstrated that the methodology presented in this paper can be used for safe and non-destructive studies of characteristic explosion products without the need for the initiation of hazardous quantities of explosives in the form of test charges. It is also interesting to note that according to preliminary experiments, the compositions of the end products of the laser-generated plasma plumes correspond well to the composition of the fumes collected after the explosion of much larger (0.5 kg) charges [30]. Therefore, we can suggest that the results of the present study are relevant to analysing gaseous residues of the explosion or combustion of real explosives and propellants.

References

1.   R. Matyáš and J. Pachman, Springer, Berlin
Heidelberg, 2013, DOI: 10.1007/978-3-642-28436-6.
2.   P. Politzer and J. S. Murray, *Energetic materials. Pt. 2, Detonation, combustion.*, Elsevier, London, 2003.
3.   S. Kolkoori, N. Wrobel, S. Hohendorf, B. Redmer and U. Ewert, *Materials Evaluation*, 2015, 73, 175-185.
4.   Z. D. Whetstone and K. J. Kearfott, *Journal of Radioanalytical and Nuclear Chemistry*, 2014, 301, 629-639.
5.   M. S. Macias, R. J. Harper and K. G. Furton, *Am. Biotechnol. Lab.*, 2008, 26, 26-27.
6.   L. A. Skvortsov, *Journal of Applied Spectroscopy*, 2014, 81, 725-749.
7.   J. Akhavan, The Royal Society of Chemistry, Cambridge, 2004, DOI: 10.1039/9781847552020.
8.   K. G. Furton, J. R. Almirall, M. Bi, J. Wang and L. Wu, *J. Chromatogr. A*, 2000, 885, 419-432.
9.   N. F. P. Association and N. F. P. Association, *NFPA 921, Guide for Fire and Explosion Investigations*, National Fire Protection Association, 2008.
10.   Y. M. Taha, C. A. Odame-Ankrah and H. D. Osthoff, *Chemical Physics Letters*, 2013, 582, 15-20.
11.   S. K. Jha, Y. Ekinci, M. Agio and J. F. Loeffler, *Analyst*, 2015, 140, 5671-5677.
12.   J. S. Li, B. Yu, H. Fischer, W. Chen and A. P. Yalin, *Rev. Sci. Instrum.*, 2015, 86.
13.   M. Ferus, J. Cihelka and S. Civiš, *Chemicke Listy*, 2008, 102, 417-426.
14.   V. Swayambunathan, G. Singh and R. C. Sausa, *Appl. Opt.*, 1999, 38, 6447-6454.
15.   I. Malka, A. Petrushansky, S. Rosenwaks and I. Bar, *Applied Physics B-Lasers and Optics*, 2013, 113, 511-518.
16.   S. Bell, in *Explosives In Forensic Chemistry*, Pearson Prentice Hall: Upper Saddle River, New Jersey, 2006.
17.   S. Meyers and E. S. Shanley, *J. Hazard. Mater.*, 1990, 23, 183-201.
18.   L. J. Radziemski and D. A. Cremers, John Wiley & Sons, West Sussex, England, 2006.
19.   M. Civiš, S. Civiš, K. Sovova, K. Dryahina, P. Spanel and M. Kyncl, *Analytical Chemistry*, 2011, 83, 1069-1077.
20.   K. Sovova, K. Dryahina, P. Spanel, M. Kyncl and S. Civiš, *Analyst*, 2010, 135, 1106-1114.
21.   M. Ferus, R. Michalcikova, V. Shestivska, J. Sponer, J. E. Sponer and S. Civiš, *Journal of Physical Chemistry A*, 2014, 118, 719-736.
22.   P. Španěl and D. Smith, *Mass Spectrometry Reviews*, 2011, 30, 236-267.
23.   D. Smith and P. Španěl, *Mass Spectrometry Reviews*, 2005, 24, 661-700.
24.   P. Španěl and D. Smith, *Mass Spectrom. Rev.*, 2011, 30, 236-267.
25.   D. Smith, A. Pysanenko and P. Španěl, *Int. J. Mass Spectrom.*, 2009, 281, 15-23.
26.   P. Španěl, K. Dryahina and D. Smith, *Int. J. Mass Spectrom.*, 2006, 249, 230-239.
27.   D. Smith and P. Španěl, *Analyst*, 2011, 136, 2009-2032.
28.   T. W. E. Chippendale, F. J. Gilchrist, P. Spanel, A. Alcock, W. Lenney and D. Smith, *Analytical Methods*, 2014, 6, 8154-8164.
29.   M. Ferus, P. Kubelik, K. Kawaguchi, K. Dryahina, P. Spanel and S. Civiš, *Journal of Physical Chemistry A*, 2011, 115, 1885-1899.
30.   K. Dryahina, in *17th Symposium on Application of Plasma Processes Visegrad Workshop on Research of Plasma Physics*, ed. S. Matejcik, Liptovský Ján, Slovakia, 2009.

1
2
3
4
5
6
7
8
9
10
11
12
13
14
15
16
17
18
19
20
21
22
23
24
25
26
27
28
29
30
31
32
33
34
35
36
37
38
39
40
41
42
43
44
45
46
47
48
49
50
51
52
53
54
55
56
57
58
59
60

1
2
3
4
5
6
7
8
9
10
11
12
13
14
15
16
17
18
19
20
21
22
23
24
25
26
27
28
29
30
31
32
33
34
35
36
37
38
39
40
41
42
43
44
45
46
47
48
49
50
51
52
53
54
55
56
57
58
59
60